Three phase converter with galvanic isolation based on loss-free resistors for HB-LED lighting applications

Ignacio Castro, Diego G. Lamar, Manuel Arias and Javier Sebastián
Departamento de Ingeniería Eléctrica, Electrónica, de Computadores y Sistemas
University of Oviedo
Gijón 33204, Spain
e-mail: castroignacio@uniovi.es

***Abstract*—This work presents a driver for High-Brightness Light-Emitting Diodes (HB-LED) in three-phase grids, which complies with IEC 1000-3-2 Class C requirements, achieves high Power Factor (PF), low harmonic distortion, as well as, the capability to achieve full dimming while disposing of the bulk capacitor and having galvanic isolation. The HB-LED driver is based on the use of six two-port cells with their inputs connected to the three-phase network and their outputs connected in parallel. Each one of these cells is a DC/DC converter operating as a Loss-Free Resistor (LFR) based on the concept of a flyback working in Discontinuous Conduction Mode (DCM). Moreover, it works in the full range of the European three-phase line voltage, which varies between 380V and 420V, and it supplies an output voltage of 48V with maximum power of 90W.**

***Keywords*—Three-phase, PFC, HB-LED driver, LFR.**

I. INTRODUCTION

Light emitting diodes (LED) are becoming increasingly ubiquitous across all aspects of illumination products, by offering a lot of advantages over traditional lighting solutions. Furthermore, several commercial and industrial installations around the globe receive primary three-phase power with a wide variety of voltages depending on the country, e.g. line-neutral is 347V in Canada, 480V in the US or 230V in the European Union with the exception of the UK (240V). Hence, one question arises, why is not a specific solution for LEDs used in three-phase grids.

High-Brightness Light-Emitting Diodes (HB-LED) drivers are normally designed for single-phase universal input voltage supplies (100 to 277V). Therefore, the use of these LED drivers in installations with exclusive access to three-phase requires a step-down autotransformer, as well as, access to neutral [1]. The use of these step-down autotransformers reduces the efficiency of the whole system greatly due to their electrical efficiency not being higher than ~95% in a best case scenario. Another aspect that needs to be taken into account is the size increase of the power supply [2]. Hence, the necessity of a compact solution especially designed for this specific application.

In prior literature, there are several works dedicated to the study of AC/DC three-phase power supplies, synthesized in [3]. Most of the converters based on a single switch have high power factor (PF) by penalizing the Total Harmonic Distortion (THD) or having the need of high output voltage. In order to have high PF and not to penalize THD, it will be necessary to use a three-phase driver based on multi-cell loss free resistor (LFR). These drivers are more complex from a control point of view since they add more components and are arguable more expensive, but they have a better trade-off between the output voltage and THD. There are only a handful of these converters in literature, based on DCM flybacks [4] [5], Cùk [6], SEPIC [7], used as LFR cells. This digest proposes the use of this type of multi-cell converter as HB-LED driver. It should be noted that, the use of any three-phase converter with unity PF means that the output power is not pulsating, therefore allowing not only to remove the electrolytic capacitor in commercial and industrial installations, but also to increase the light quality in these environments.

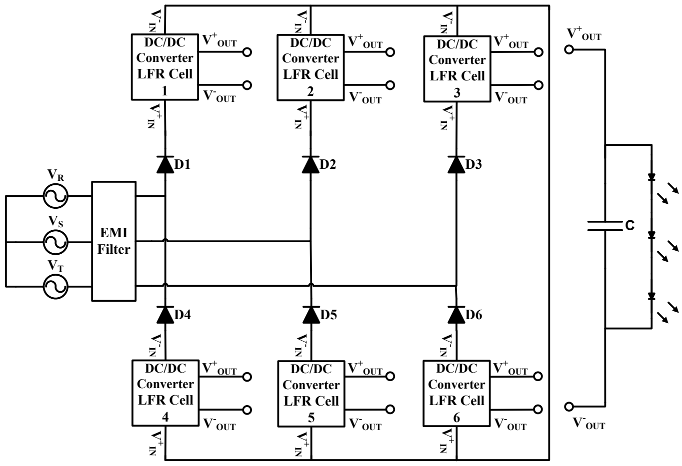

Fig 1. Diagram of the multi-cell three-phase HB-LED driver.

In order to design this driver the IEC 1000-3-2 [8-10] regulation is going to be taken into account. However, it is not a simple task to fit a three-phase power supply for lighting applications in the classes (A, B, C and D) specified in the regulation. It should be classified as Class A equipment taking into account that it is three-phase equipment, but it should comply with Class C taking into account that it is also lighting equipment. Therefore, the aim of this work will be for the HB-LED driver to comply with the more restrictive of the two which is Class C.

It should be noted that some work has been done previously in the field of three-phase dimmable lightning, in this case for fluorescent lamps [11]. Although, it has never been done for LED lighting. In this paper, a compact HB-LED dimmable driver is proposed, based on the idea of [5] by using LFR cells as it is illustrated in Fig. 1, which will be extensively described in Section II. Section III will be dedicated to the control of said

This work has been supported by the Asturian Gobernment through the grant Beca Predoctoral "Severo Ochoa" BP14-140, by the Spanish Ministry of Education and Science under Consolider Project RUE CSD2009-00046 and under Project DPI2013-47176-C2-2-R, by the University of Oviedo under the Project UNOV-13-EMERG-GIJON-12 and by European Regional Development Fund (ERDF) grants.

converter, and finally Section IV will synthesize the most relevant experimental results.

In summary, the use of three-phase AC/DC converters instead of single-phase ones makes possible to remove the most critical device from the point of view of the converter lifespan: the electrolytic capacitor. The price to pay is to connect the LED driver to a 3-wire line instead of a 2-wire one.

II. PROPOSED LED DRIVER

The concept of the HB-LED driver presented in this work is depicted in Fig. 1, based on a family of three-phase power supplies which are built with LFR, in order to achieve high quality rectification [4]. The one presented in this work is based on the idea of [5].

Each one of the cells depicted in Fig. 1, is a DC/DC converter working as a LFR. The proposed cells in this case are flyback converters working in DCM, as shown in Fig. 2.

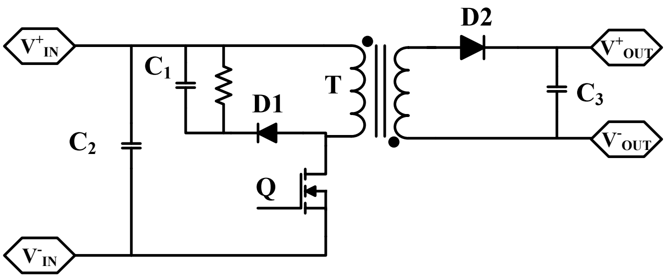

Fig 2. Schematic of the LFR flyback cell.

As has been stated in [12], a flyback working in DCM supplies a fixed amount of current to the load, which in this case are HB-LED. The LFR of a DCM flyback converter, which is the basic cell, can be defined by:

$$R_{cell} = \frac{2L}{D^2 T}, \qquad (1)$$

where D is the duty cycle of the converter, L is the magnetizing inductance of the transformer and T is the switching period. By forcing the flybacks to work in DCM with a fixed duty cycle, it can be assured that each one of the flybacks behaves as a resistor at their input. Hence, each phase will demand a sinusoidal current granting both high PF and low THD.

Henceforth, to simplify the analysis of the HB-LED driver, the LFR cells are going to be considered as ideal resistors. Their value is going to be considered equal not taking into account tolerances that could come from the components.

In order for the HB-LED driver to demand a sinusoidal current, each one of the diodes is going to be conducting during half line cycle. Hence, three different diodes are going to be conducting every 60º, depending on the phase voltages (V_R, V_S, V_T), as it is summarized in Fig. 3. For instance, D_2 conducts during the positive half line cycle of line S, from t_1 to t_4, as stated in Fig. 3. At the time, there are two other diodes conducting. However, they do not share the same conduction time as D_2 (t_1, t_4) meaning there is a different set of three diodes conducting every 60º.

Therefore, the driver can be divided in three stages for each one of the diodes. These three stages are depicted as an example for diode D_2 in Fig. 4 (a), (b) and (c), where D_2 is the diode that is conducting from t_1 to t_4 and D_1, D_3, D_4 and D_6 are the diodes that are swapping in between depending on the voltages of phases R and T.

The analysis done for D_2 is equivalent for the rest of the diodes. Hence, if the whole line period where to be considered, the HB-LED driver is equivalent to a star connection (Y), as shown in Fig. 3 (d), meaning that the input current of each phase (I_{phN}) of the converter is going to be defined by:

$$I_{phN} = \frac{V_N}{R_{cell}} = \frac{V_p}{R_{cell}} \cos(\omega t - \varphi_N), \qquad (2)$$

where V_N is the phase-neutral voltage of one of the phases (N defines whether is phase R, S or T), Vp is the peak amplitude of the phase-neutral voltage and φ_N is the phase of the signal.

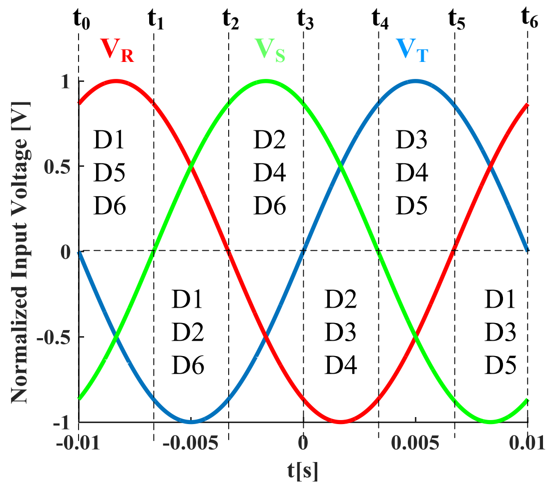

Fig 3. Theoretical conduction of the diodes depending on the phase voltages.

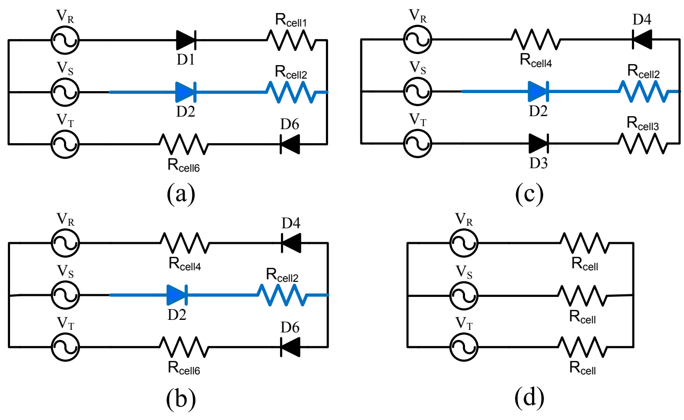

Fig 4. (a) Conduction during [t1, t2] (b) Conduction during [t2, t3] (c) Conduction during [t3, t4] (d) Simplified working behaviour of the driver.

Assuring unity factor power correction allows not to have pulsating power at the HB-LED driver input. Therefore, the input power of the converter will be defined by the sum of each phase, as shown in (3), since only three of the six cells are going to be working at the same time.

$$P(t) = \sum_{i=1}^{3} \frac{V_N^2}{R_{cell}} = \frac{3V_p^2}{2R_{cell}} = \frac{3V_p^2 D^2 T}{4L} \quad (3)$$

It should be noted, that the sinusoidal components that come out from the summation in (3) can be removed due to their sum being equal to zero. Hence, the input power of the converter can be defined by a DC component.

From Figure 4, it can be observed that the line currents undergo the voltage drop corresponding to only three rectifier diodes, which is an important advantage over the topology proposed in [4], where the line currents undergo the voltage drop corresponding to six rectifier diodes.

Regarding the connection of the outputs, every single one of the LFR cells needs to be connected in parallel to the same load. Accordingly, if the simplification from Fig 3. (d) is taken into account with the parallel output connection, Fig. 5 can be derived. In this figure the basic operation of the converter is explained with the three active cells that are feeding the LED string keeping in mind the cell behaviour as a power source.

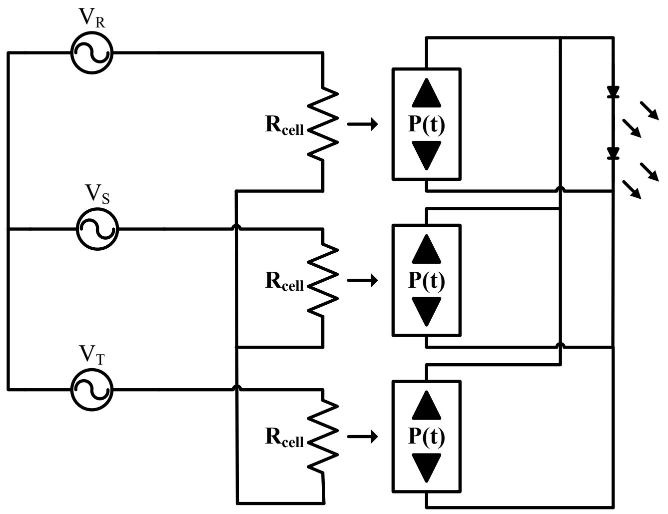

Fig 5. Three-phase HB-LED driver simplified with LFR.

The parallel output connection allows the complete removal of the bulk capacitor due to the non-pulsated power given to the load. Hence, a film capacitor can be used to reduce the switching frequency ripple, which is the only ripple at the HB-LED driver output. Furthermore, being able to eliminate the bulk capacitor from the HB-LED driver, increases dramatically the lifespan of the driver. Particularly important for lighting environments with either difficult access or expensive solutions that need to guarantee a high lifespan of the driver.

Therefore, if non-pulsated power given to the load is considered and a relation is made between input power (3) and output power, equation (4) is derived:

$$P(t) = \frac{3V_p^2}{2R_{cell}} = \frac{V_o^2}{R_L} \rightarrow \frac{V_o}{V_p} = \sqrt{\frac{3R_L}{2R_{cell}}}, \quad (4)$$

where V_O is the output voltage and R_L is the load resistance.

From (4) the duty cycle required to drive the HB-LED driver can be obtained, considering the same PWM signal is going to be driving all the flybacks, as has been stated in (5):

$$D = \frac{2V_O}{V_p}\sqrt{\frac{L}{3R_L T}} \quad (5)$$

Full dimming on the LED is achieved by reducing the duty cycle, which increases the emulated resistance diminishing the output current while keeping theoretical sinusoidal input current.

From the design point of view, the designer needs to calculate both the theoretical duty cycle (5) and the maximum output power (3) required for its specifications. Afterwards, the LFR flyback cell needs to be designed, as has been explained in previous literature [12], considering an input voltage in the cells equal to the one of the phase-neutral. Furthermore, the designer needs to keep in mind that each flyback is going to handle one sixth of the input power.

III. Control Strategies

Closed loop operation is mandatory in most applications where a certain voltage or current levels needs to be guaranteed at the output. HB-LED drivers are no exception, meaning a certain voltage/current level needs to be assured in order to guarantee not only, good light quality but to avoid harmful effects for human beings in an industrial environment.

From the schematic depicted in Fig. 5, the control of the HB-LED driver can synthesized as a problem of three power supplies connected in parallel to the same load. Many works in previous literature have address the parallelization of powers supplies and are synthesized in [13-15]. From these works a quick conclusion can be extracted: the most optimal way to control the power supplies (LFR cells) would be for each one of them to have their own control current loop. However, in our case of study that means the use of a current sensor for each cell, which leads to

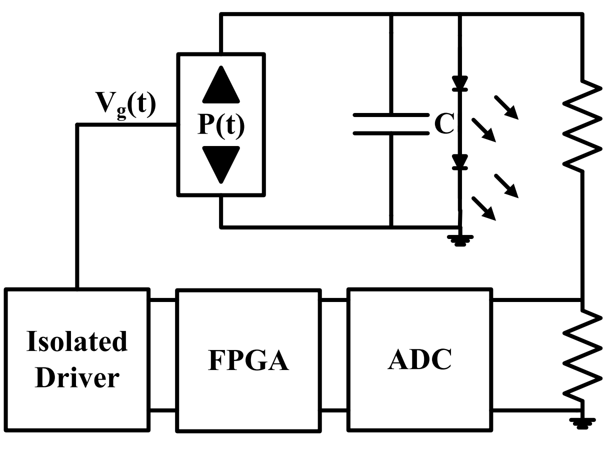

Fig 6. HB-LED driver voltage loop diagram.

six current sensors. This soulution would increase not only the price but the complexity of the control. Hence, a voltage loop like the one depicted in Fig. 6 is going to be used.

It is important to note that the tolerances of the components are going to have an effect over the LFR value (R_{cell}). Especially the tolerance of L which is the most critical component in this sense. This variation of the R_{cell} from one cell to another will have an effect on the output voltage of the converter. Therefore, an independent current control for each cell would be optimal to reduce the tolerance effects or any unbalance that could come from the three-phase grid. However, since the change between R_{cell} are really small, it does not justify the use of a more complex control.

The voltage loop proposed in Fig. 6, is going to be based on measuring the output voltage by means of a voltage divider. That voltage is going to be digitally converted and processed by an FPGA, in order to generate the digital pulse-width modulation (DPWM) that goes to the isolated driver of each cell. The signal that goes into each isolated driver is $V_g(t)$, and is the same signal for the switch of each cell.

In order to determine the compensator to be used in the HB-LED driver, the plant of the HB-LED driver needs to be calculated using a similar analysis to the one done in [4] by using Ridley's average small signal analysis [16]. Consequently, the starting point for this analysis would be the input power handled by the HB-LED driver and defined by (3) and the equation that can be obtained from the circuit in Fig. 6 defined by (6) considering the HB-LED string as a resistor:

$$P(t) = CV_o(t)\frac{dV_o(t)}{dt} + \frac{V_o^2(t)}{R_L} \tag{6}$$

By equating both (3) and (6), (7) is derived. It should be noted, that both V_p and D are dependent on time. The first one due to the variations that can occur in a three-phase grid and the second one due to the variation that the loop is now able to do to the duty cycle in order to regulate the output voltage.

$$\frac{3V_p^2(t)D^2(t)T}{4L} - CV_o(t)\frac{dV_o(t)}{dt} - \frac{V_o^2(t)}{R_L} = 0 \tag{7}$$

After perturbing equation (7), and eliminating the second order and the DC terms, equation (8) is reached.

$$\frac{3V_p^2DT}{2L}\hat{d} + \frac{3V_pD^2T}{2L}\hat{v}_p - CV_o\frac{d\hat{v}_o}{dt} - \frac{2V_o}{R_L}\hat{v}_o = 0 \tag{8}$$

Then, the Laplace transform of (8) needs to be performed in order to yield (9) and (10).

$$G_{v_od}(s) = \left.\frac{\hat{v}_o(s)}{\hat{d}(s)}\right|_{\hat{v}_p=0} = \sqrt{\frac{3R_LT}{L}}\frac{V_P}{\left(\frac{CR_Ls}{2}+1\right)} \tag{9}$$

$$G_{v_ov_p}(s) = \left.\frac{\hat{v}_o(s)}{\hat{v}_p(s)}\right|_{\hat{d}=0} = \frac{V_o}{V_P\left(\frac{CR_Ls}{2}+1\right)} \tag{10}$$

It should be noted that equations (9) and (10) are valid, if and only if, the compensator has a crossover frequency of less than 300Hz, that guarantees that there is no frequency component having an effect over the control action. This is extremely important, because when closing the loop, the power supply can vary the value of the R_{cell}, meaning that this will have an impact on the THD. So if rapid changes are allowed the unity factor correction that assures almost DC current at the output might not be guaranteed.

IV. Experimental Results

The HB-LED driver introduced in the previous sections has been designed for a maximum power of 90W. This driver receives a three-phase input of 400V line-to-line and feeds five strings of 12 HB-LED (W42180T2-SW) that are equivalent to 1.8A/48V at full load. The switching frequency of each flyback is 100 kHz. Moreover, the LFR cell is based on a flyback converter working in DCM, as the one shown in Fig. 2 and whose components are summarized in Table I. Each one of these flybacks handles one sixth of the total power as it was previously stated, meaning that each one handles 15W. The rest of the components that form the HB-LED driver are summarized in Table II. Finally, Fig. 7 shows a picture of the prototype that was built to validate the concept of this work. It should be noted that the flyback transformers are on the other side of the board.

TABLE I. Components of the Experimental LFR cell prototype

Fig. 2 reference	Value
D_1	STTH208U
D_2	FES8BT-E3/45
C1	1µF 800V Ceramic Cap.
C2	100nF 50V Film Cap.
C3	1µF 50V Film Cap.
R	10.5kΩ
Q	IPP65R225C7
T	Coilcraft Z9007-BL

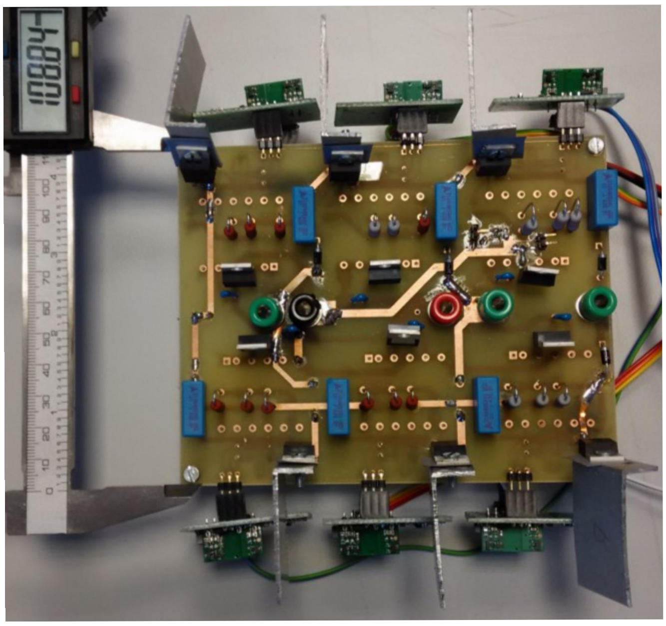

Fig 7. HB-LED driver prototype.

TABLE II. REST OF COMPONENTS OF THE HB-LED DRIVER

Fig. 1 reference	Value
D_1-D_6	1N4007
C_o	10µF 100V Film Cap.
FPGA	XC7A100T-1CSG324C

All the tests have been done connected to the real three-phase power grid, which justifies the distortion of V_R in Fig. 8. In the same figure, a snapshot of the oscilloscope is shown where the input currents of the driver, as well as, one of the phase-neutral input voltages of the converter can be observed. As it can be seen, the current (I_R) follows the voltage (V_R) demonstrating that power factor correction is achieved. The phase shift between currents is 120º, so it can be assumed that power correction in the three phases is achieved. In Fig. 9, it can be observed that both the output current and the output voltage have low ripple with a 10µF film capacitor.

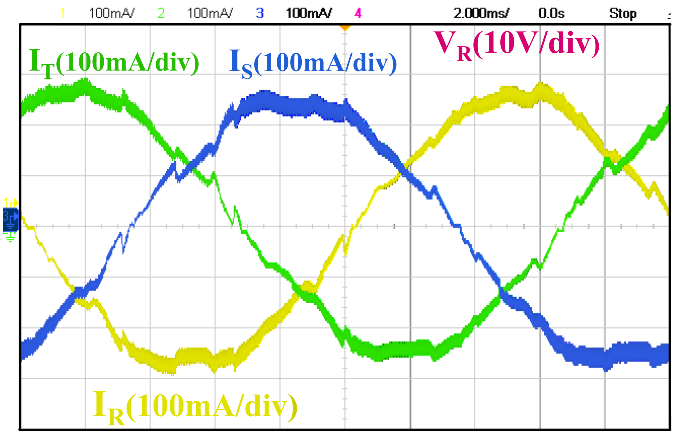

Fig 8. Input currents for all three phases and input voltage of phase R when fully loaded.

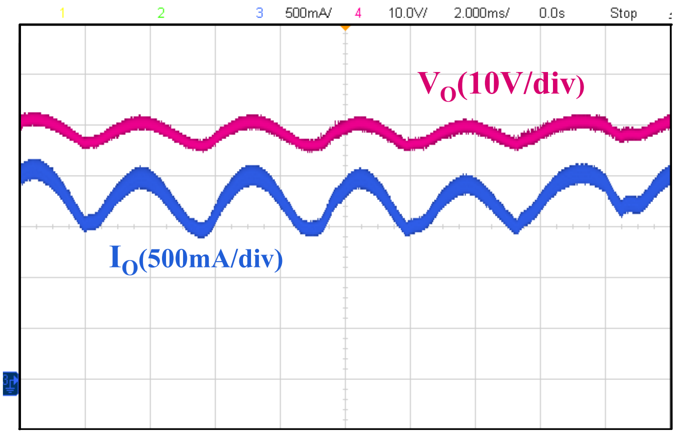

Fig 9. Output current and output voltage when fully loaded.

In order to validate the HB-LED driver, several measurements are going to be taken into account. Firstly, to validate the dimming of the HB-LED driver, three operating points are going to be measured by varying the voltage reference of the loop, therefore, varying the output current to

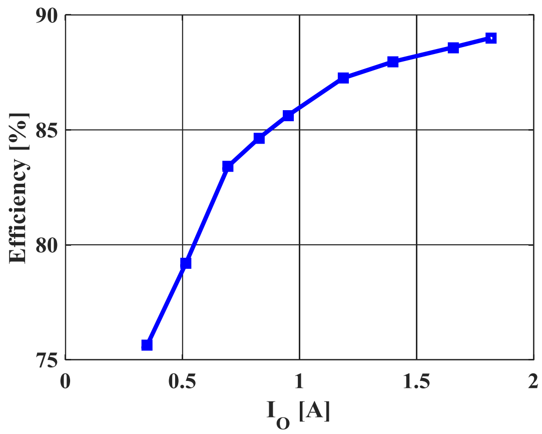

Fig 10. Efficiency of the LED driver versus output current.

1.8A (fully loaded), 0.9 A (full dimming condition) and 0.45 A. Secondly, the HB-LED driver needs to work in the full range of the European three-phase voltage line meaning that also three operating points are going to be measured, 380, 400 and 420V_{rms}.

To correctly analyze the waveforms in both scenarios, the waveforms are going to be extracted from the oscilloscope as data and processed with MATLAB®. The parameters that are going to be extracted for each one of the points are: efficiency, THD, PF, compliance with Class C IEC 1000-3-2 [9-11] for both, and flicker operating recommendation [18][19] for the dimming validation.

A. Dimming validation of the HB-LED driver.

The dimming validation is shown in Table III, which summarizes PF and THD measurements for each phase based on input voltages and input currents extracted from the oscilloscope for the three operating points stated before, which are 1.8A, 0.9A and 0.45A. It can be observed that THD increases and PF decreases, when lowering the output current by diminishing the duty cycle of the power supply. As for the efficiency of the HB-LED driver, in Fig. 10 it can be seen that it decreases by lowering the output current, being roughly 86% at the full dimming point (0.9A).

The efficiency of the HB-LED driver is 88% at full load. It should be noted that the efficiency of the driver was not the aim of this work, since it was proving the concept of feeding HB-LED in three-phase power grids. The efficiency of the HB-LED driver is completely reliant on the efficiency of each cell (flyback). In fact, it will be the efficiency of the cell affected by the voltage drop corresponding to the rectifier diode associated

TABLE III. COMPONENTS OF THE EXPERIMENTAL LFR CELL PROTOTYPE

Output Current/Phase		1.8A	0.9A	0.45A
R	PF[%]	99.81	99.72	99.56
	THD[%]	5.71	6.97	8.03
S	PF[%]	99.87	99.75	99.59
	THD[%]	4.62	6.96	7.71
T	PF[%]	99.85	99.73	99.58
	THD[%]	5.26	6.86	7.97

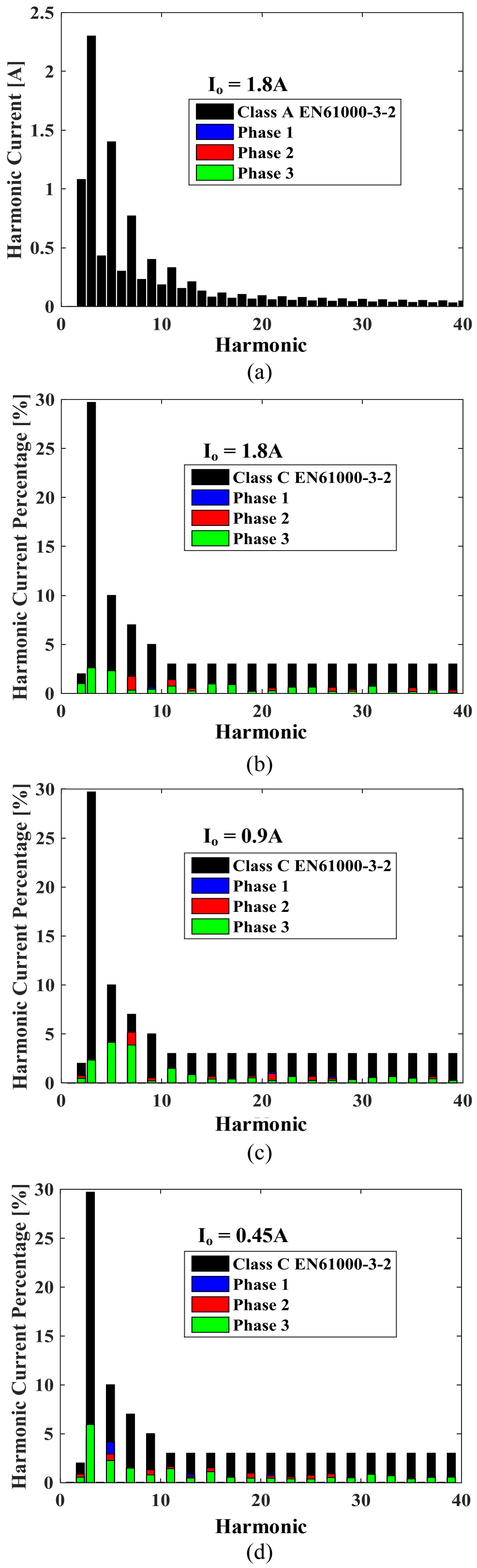

Fig 11. Harmonic content of each phase compared with both Class A and Class C limits. (a) Class A comparison for 1.8A. (b) Class C comparison for 1.8A (c) Class C comparison for 0.9A (d) Class A comparison for 0.45A.

The waveforms have also been used to extract the harmonics by using the Fourier series on them. Afterwards, these measurements are compared with Class A IEC 1000-3-2 harmonic limits, since it is the category a balanced three phase converter, as the one shown in this work, falls in the regulation. However, the measured harmonics are so low they do not appear in Fig. 11(a) for the 1.8A measurement and they do not appear either for the other two values under study due to their current being even lower. Hence, it seemed interesting to test the compliance of Class C IEC 1000-3-2 harmonic limits for each phase and each operating point considering the presented power supply as a HB-LED driver. Fig. 11 (b), (c) and (d) show the compliance with said regulation.

As it can be seen in Fig. 12, even in full dimming conditions the output current and voltage have low ripples by penalizing in this case both the efficiency and THD, as have been shown before.

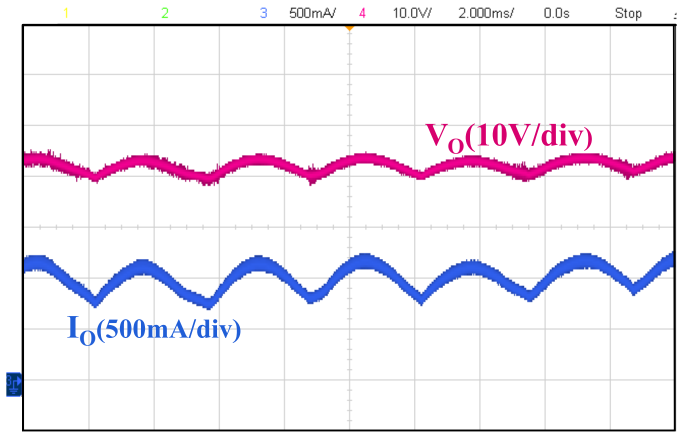

Fig 12. Output current and output voltage in full dimming.

To limit the biological effects and detection of flicker in general illumination, the Modulation (%) should be kept within the shaded region defined in [18][19], where Modulation(%) calculation can be define as follows:

$$Modulation\ (\%) = 100 \cdot \frac{(L_{max} - L_{min})}{(L_{max} + L_{min})}, \qquad (12)$$

where L_{max} and L_{min} correspond to the maximum and minimum luminance of each harmonic of the ac component of the output current, respectively.

In this case a proportionality between luminance and the ac component of output current has been assumed. Results of this analysis are shown in Fig. 13 for the three operating points under study. As you can see, all ac harmonic content is within the shaded region. Therefore, good light quality and non-harmful effects can be assumed from the HB-LED driver presented, even in full dimming conditions.

B. Input voltage range validation.

The European three-phase voltage standard is $230V_{rms}$ phase-neutral and a variation of 10%, except for the UK, Malta and Cyprus which is $240V_{rms}$ [20]. As in this previous subsection three points are going to be considered to validate the operation

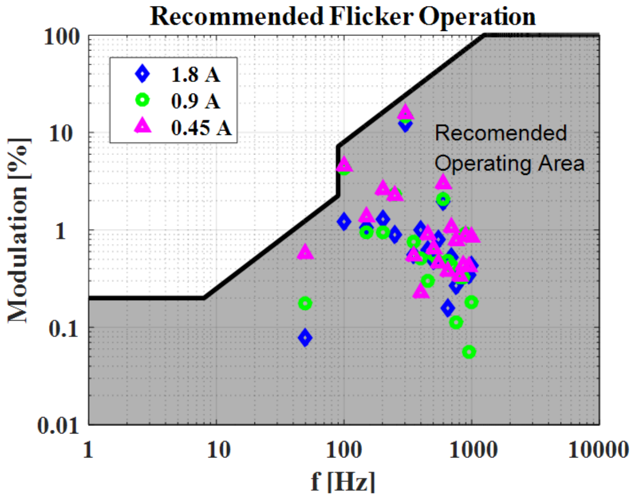

Fig 13. Recommended flicker operation, P1789 [18].

of the HB-LED driver, in this case those are 380V, 400V and 420V line-to-line RMS. However, only the THD, PF and efficiency are going to be shown since the compliance with class C was already demonstrated in the previous subsection and this low variation have next to none effect over the other parameters. The first two parameters are shown in Fig. 14, where it can be seen that THD increases with the input voltage. This is due to the voltage loop lowering the duty cycle in order to regulate the voltage. It should also be noted that the prototype complies with ENERGY STAR regulations [21].

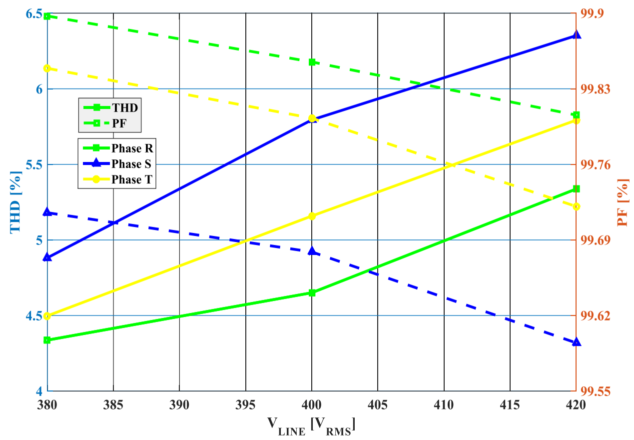

Fig 14. Evolution of the PF, THD versus the line input voltage.

As for the efficiency, the results are shown in Fig. 15. In this case the efficiency of the converter have been measured in several operating points using a resistor instead of the HB-LED.

C. *Detailed description of the designed voltage loop.*

In this subsection the designed compensator for the voltage loop is going to be explained. For that reason, in Fig. 16 there is a detailed diagram of said voltage loop.

It is important to note that the compensator is designed for a digital control. Therefore, limit cycling needs to be taken into account in the design of the compensator, in this case by using

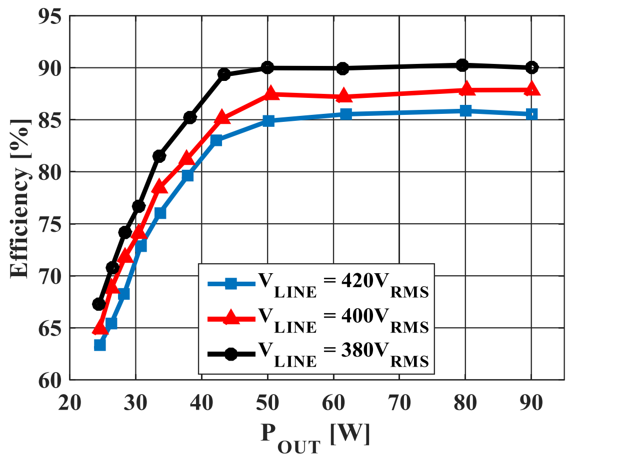

Fig 15. Evolution of the efficiency with input line voltage and the load.

the definitions that guarantee non limit cycling in PFC [17]. Moreover, the design shown in (11) with a very simple compensator has settling time of roughly 4ms. This compensator satisfies the requirements stated at the end of the previous subsection while having a phase margin of 80.7º, as it is shown in Fig. 17.

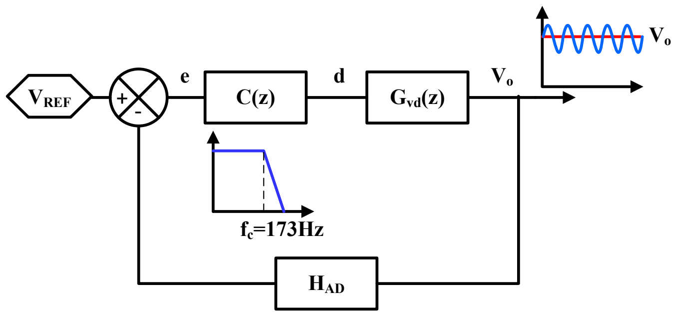

Fig 16. Block diagram of the digital control loop.

$$C(z) = \frac{0.2(z+1)}{(z-1)} \quad (11)$$

The tests done to validate the voltage loop are executed with a resistive load going from full load (90W) to half load (45W) and vice versa. These tests are depicted in Fig. 18 (a) and (b), where it can be seen that when a load transient is applied, not only is the voltage loop able to correct the output voltage but the settling time matches the 4ms corresponding with the one that was obtained from doing the dynamic analysis of the HB-LED driver.

It should be noted that these tests are done for the sake of completion of the voltage loop analysis and they are not crucial from the point of view of the stability and dynamic response of a load composed of HB-LED.

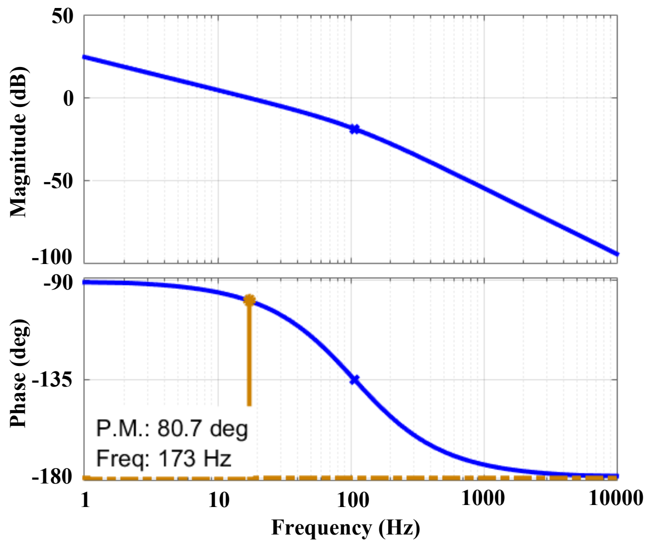

Fig 17. Bode diagram in open loop.

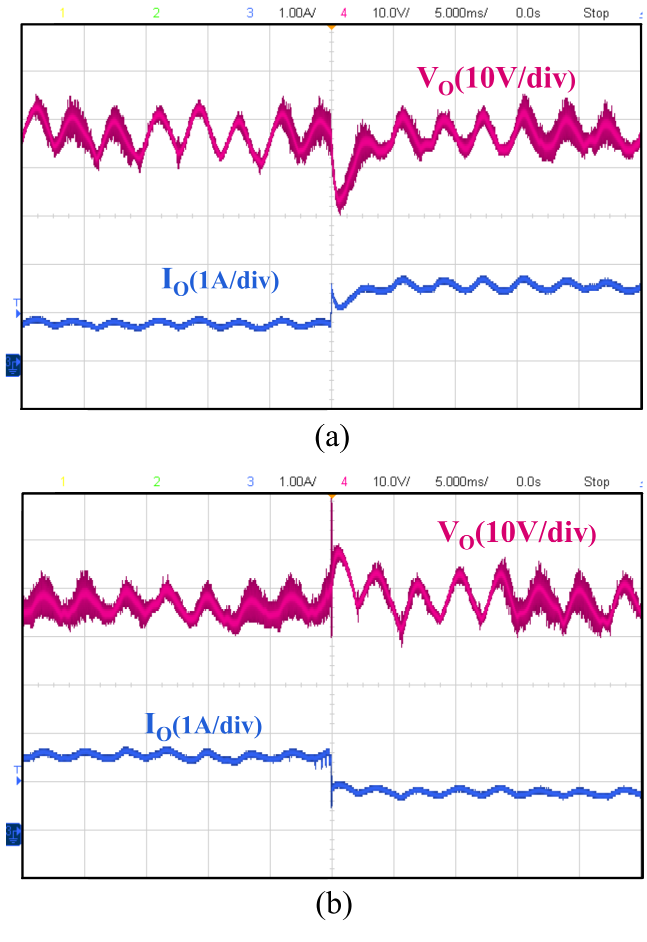

Fig 18. Load transient response of the HB-LED driver. (a)Half load to full load. (b) Full load to half load.

V. CONCLUSIONS AND FUTURE WORK

A three-phase HB-LED driver has been reported and experimentally proven in this work. The HB-LED driver under study provides high PF and low THD and compliance with Class C IEC 63000-3-2. The analysis carried out over different dimming operating shows a non-flicker behaviour from a health point of view, while disposing of the traditional bulk capacitor in power factor correction. The disposal of said capacitor increases greatly the lifespan of the HB-LED driver making it a great solution for lighting in primary three-phase grids.

The driver has been tested in the whole range of European three phase voltage, showing lower efficiencies for the higher values of the range but still being a valid solution, taking into account that THD and PF roughly vary in this analysis.

Finally, the voltage loop has been validated with a couple of transient loads with the use of resistive loads. In this regard more work will be done in the future by looking at different controls or different LFR setups that can help reduce the ripple of both output voltage and current.

REFERENCES

[1] Gray, G.; “Demystifying 347V and 480V Lighting Installations,” e-Craftsmen.

[2] “480V to 277V Step-Down Autotransformers For applications up to 375 Watts”, GE lighting.

[3] Singh, Bhim; Singh, B.N.; Chandra, A.; Al-Haddad, K.; Pandey, A.; Kothari, D.P., "A review of three-phase improved power quality AC-DC converters," Industrial Electronics, IEEE Transactions on , vol.51, no.3, pp.641,660, June 2004

[4] Singer, S.; Fuchs, A., "Multiphase AC-DC conversion by means of loss-free resistive networks," Circuits, Devices and Systems, IEE Proceedings - , vol.143, no.4, pp.233,240, Aug 1996

[5] “High Power Factor Modular Polyphase AC/DC converters based on Loss-Free Resistors”, Paper submitted for APEC '16, Applied Power Electronics Conference and Exposition, 2016.

[6] Kamnarn, U.; Chunkag, V., "Analysis and Design of a Modular Three-Phase AC-to-DC Converter Using CUK Rectifier Module With Nearly Unity Power Factor and Fast Dynamic Response," Power Electronics, IEEE Transactions on , vol.24, no.8, pp.2000,2012, Aug. 2009

[7] Tibola, G.; Barbi, I., "Isolated Three-Phase High Power Factor Rectifier Based on the SEPIC Converter Operating in Discontinuous Conduction Mode," in Power Electronics, IEEE Transactions on , vol.28, no.11, pp.4962-4969, Nov. 2013

[8] Draft of the Proposed CLC Common Modification to IEC 61000-3-2 Document, 2006.

[9] Draft of the Proposed CLC Common Modification to IEC 61000-3-2/A2 Document, 2010.

[10] Electromagnetic Compatibility (EMC)-Part 3: Limits-Section 2: Limits for Harmonic Current Emissions (Equipment Input current < 16 A per Phase), IEC1000-3-2, 1995.

[11] Sabahi, M.; Hosseini, S.H.; Sharifian, M.B.B.; Goharrizi, A.Y.; Gharehpetian, G.B., "A Three-Phase Dimmable Lighting System Using a Bidirectional Power Electronic Transformer," Power Electronics, IEEE Transactions on , vol.24, no.3, pp.830,837, March 2009

[12] Erickson, R.; Madigan, M.; Singer, S., "Design of a simple high-power-factor rectifier based on the flyback converter," Applied Power Electronics Conference and Exposition, 1990. APEC '90, Conference Proceedings 1990, Fifth Annual, vol., no., pp.792,801, 11-16 March 1990

[13] Glaser, J.S.; Witulski, A.F., "Application of a constant-output-power converter in multiple-module converter systems," in Power Electronics Specialists Conference, 1992. PESC '92 Record., 23rd Annual IEEE , vol., no., pp.909-916 vol.2, 29 Jun-3 Jul 1992

[14] Yuehui Huang; Tse, C.K., "Circuit Theoretic Classification of Parallel Connected DC–DC Converters," in Circuits and Systems I: Regular Papers, IEEE Transactions on , vol.54, no.5, pp.1099-1108, May 2007

[15] Yuehui Huang; Tse, C.K., "Classification of parallel DC/DC converters part II: Comparisons and experimental verifications," in Circuit Theory and Design, 2007. ECCTD 2007. 18th European Conference on , vol., no., pp.1014-1017, 27-30 Aug. 2007

[16] Ridley, R.B "Average small-signal analysis of the boost power factor correction circuit", VPEC Seminar Proceedings, 1989, pp. 108-120

[17] Mather, B.A.; Maksimovic, D., "Quantization effects and limit cycling in digitally controlled single-phase PFC rectifiers," in Power Electronics Specialists Conference, 2008. PESC 2008. IEEE , vol., no., pp.1297-1303, 15-19 June 2008

[18] "RP-16-10, Nomenclature and Definitions for Illuminating Engineering", Illuminating Engineering Society.

[19] IEEE Recommended Practices for Modulating Current in High-Brightness LEDs for Mitigating Health Risks to Viewers," in IEEE Std 1789-2015 , vol., no., pp.1-80, June 5 2015

[20] IEC standard voltages, IEC60038, 1983.

[21] Revised ENERGY STAR Program Requirements for Solid-State Lighting Luminaires: Eligibility Criteria—Version 1.1, Dec. 2008.